Optical and structural characteristics of YAG:Sm crystals grown by HDC method in Ar+(CO, H$_2$) atmosphere

S. Nizhankovskyi, S. Kryvonogov, A. Kozlovskyi, O. Lukienko, S. Skorik, A. Romanenko, I. Pritula

Institute for Single Crystals, NAS of Ukraine, STC «Institute for Single Crystals» НАН України, Kharkov, 60 Nauki Ave. Ukraine

Yttrium-aluminum garnet crystals doped by samarium ions (YAG:Sm) were grown by the method of horizontal directional crystallization in molybdenum crucible in reducing carbon-containing medium Ar+(CO, H$_2$). Studied were the content and distribution of Sm^{3+} ions, the spectral, structural characteristics and the main types of defects of these single crystals. There was shown the possibility to obtain YAG:Sm crystals of optical quality with the concentration of samarium ions up to 7. 4 at. %, as well as the coefficient of linear optical absorption equal to 0.015 cm^{-1} and 6 cm^{-1} for the pumping and generation wavelengths of YAG:Nd crystals, respectively. Established was the existence of additional absorption bands in the UV and visible ranges caused by the reducing crystal growth conditions and formation of F$^+$- color centers.
Keywords: samarium, yttrium-aluminum garnet, molybdenum crucible, horizontal directional crystallization

Оптичні та структурні характеристики кристалів YAG:Sm вирощені методом HDC в атмосфері Ar+(CO, H$_2$). *С. Ніжанковський, С. Кривоногов, А. Козловський, О. Лукієнко, С. Скорик, А. Романенко, І. Притула*

Методом горизонтальної спрямованої кристалізації в молібденовому тиглі та відновній вуглецемісній атмосфері Ar+(CO, H$_2$) вирощені монокристали ітрій-алюмінієвого гранату, що доповані іонами Sm. Проведено дослідження вмісту та розподілу іонів Sm^{3+}, спектральних, структурних характеристик і основних типів дефектів монокристалів. Показана можливість отримання кристалів YAG:Sm оптичної якості з концентрацією іонів самарію до 7,4 ат. % та коефіцієнтом лінійного оптичного поглинання 0,015 см$^{-1}$ і 6 см$^{-1}$ для довжин хвилі накачки та генерації YAG:Nd, відповідно. Встановлено існування додаткових смуги поглинання в УФ та видимому діапазоні, які обумовлені відновними умовами вирощування та утворенням F$^+$-центрів забарвлення.

1. Introduction

Over the past few years, interest in the practical use of Sm^{3+}-doped single crystals and optical ceramics based on yttrium-aluminum garnet (YAG), has significantly increased [1]. As shown while studying the spectral properties of the composite core-doped ceramic Nd:YAG by Sm:YAG cladding, the main luminescence of Nd^{3+} ions at 1064.15 nm wavelength can be absorbed quite effectively in YAG:Sm on the side part of the absorption band of Sm^{3+} ions with a maximum at 1068 nm [2]. Moreover, YAG:Sm has a weak absorption near 808 nm (the wavelength of YAG:Nd diode pumping) on a level of ≤ 0.1 см$^{-1}$, and rather high value of figure of merit FOM=α(1064 nm)/α(808 nm), that ex-

ceeds the corresponding value in comparison with other dopants [3]. Thus, YAG:Sm can be used as an effective suppressor of parasitic oscillations in YAG:Nd caused by enhanced spontaneous emission of Nd^{3+} luminescence facilitated by the reflection from the active element faces [2, 3].

Nowadays, YAG:Sm crystals with samarium concentrations up to 5 at % are grown by the Czochralski method from iridium crucible in oxidizing medium [4]. The standard crystallization rate for YAG:Sm is ≤ 1 mm/hour, so the obtaining of the crystals in iridium crucible is an expensive process. The increase of samarium concentration over 5 at.% for raising the suppressor effectiveness is bound up with the problem of increase in the number of defects. Therefore, development of new crystal growth technologies and modification of the existing ones are topical problems. Besides the Czochralski method, for the obtaining of YAG:Sm crystals there was used the method of EFG [5]. However, the dimensions and quality of the obtained crystals are still insufficient for their application in optics. Moreover, the technologies for the obtaining of optical ceramics are being intensively developed, too. At present, there is produced the ceramics with a concentration up to 9 at.% and optical losses of about 0.07 cm^{-1} at 808 nm pumping wavelength [6].

One of promising crystal growth technologies is the method of horizontal directional crystallization (HDC). An advantage of this method is the use of inexpensive thin-wall molybdenum crucibles instead of iridium ones. The conventional HDC technology uses molybdenum and tungsten sheet screens for thermal insulation, and vacuum as a crystal growth medium, that allows to obtain crystals of optical and structural quality. Disadvantages of the vacuum technology include violation of the melt stoichiometry due to primary evaporation of aluminum oxide [7]. This leads to separation of the phases with excess yttrium ($YAlO_3$), as well as to burnout, mass transfer and contamination of the crystals with molybdenum and tungsten up to a level of $\sim 10^{-2}$ mass %. The mentioned problems are solved by using protective reducing crystal growth atmosphere based on e.g. inert argon and hydrogen. Another option is the use of carbon-containing media realized due to application of graphite construction materials and heat-insulating materials. As a result, at high temperatures residual gases form the medium based on CO and H_2 which

content is controlled by a vacuum pumping system, or by the pressure of the inert component of the growth medium. A relatively low content of oxygen-containing components in the vapor phase of the melt (O_2, AlO, AlO_2 suboxides, etc.), CO_2, H_2O, as well as of those in the growth medium, is provided by the presence of a hot graphite surface that also favors constant regeneration of the reducing components (CO and H_2). This technology was developed for the growth of large-size optical leucosapphire crystals [8], laser titanium-sapphire crystals [9], YAG:Ce, LuAG:Pr scintillators [10] and magnesium-aluminum spinel [11], etc..

The use of the reducing carbon-containing atmosphere $Ar+(CO, H_2)$ provides an essential (by 5-10 times) decrease of the rates of melt evaporation, burnout and mass transfer of the construction materials in comparison with the corresponding values for the vacuum HDC technology. The main problem in the development of «iridium-free» technology for the growth of yttrium-aluminum garnet in reducing media is creation of the conditions for the obtaining of crystals with high optical and structural perfection. Under such growth conditions there exists a probability of formation of bubbles, inclusions, light scattering and anionic non-stoichiometry of the crystals [12].

The goal of the present work was the obtaining of YAG:Sm crystals by the method of horizontal directional crystallization in carbon-containing $Ar+(CO, H_2)$ atmosphere in molybdenum crucible, study of the content and distribution of samarium, and characterization of the defect structure, optical and spectral properties of these crystals.

2. Experimental

The starting material for the growth of the crystals was the stoichiometric mixture of the oxides with the general composition $(Y_{1-x}Sm_x)_3Al_5O_{12}$, where $x \leq 0,1$, i.e. up to 10 at.% of Sm as against yttrium. As a source of samarium ions, there was used Sm_2O_3 (99.99 mass %). The charge was obtained by the method of solid state synthesis from yttrium, samarium and aluminum oxides (99.999 mass %), according to the chemical reaction:

$$3(1-x)Y_2O_3 + 5Al_2O_3 + 3xSm_2O_3 \rightarrow 2 (Y_{1-x}Sm_x)_3Al_5O_{12}$$
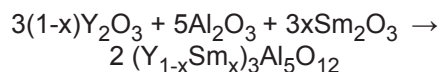
To fill the crucible more tightly, the charge was produced in the form of tablets annealed at 1200 °C.
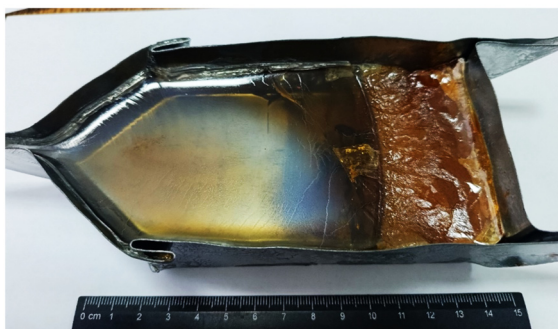
Fig. 1. YAG:Sm crystal grown by HDC method in reducing Ar + (CO, H$_2$) atmosphere

For the growth of YAG:Sm crystals by the method of horizontal directional crystallization, there was used an industrial crystal growth setup of "Gorizont-3M" type. It allows to obtain hard-melting oxide crystals with working temperatures up to 2200 °C. The crystals were obtained at the crystallization rate close to 0.5-1 mm/h in the medium of Ar+(CO, H$_2$), the general pressure was 0.11 MPa, the content of the reducing components being up to 1 vol.%.

3. Results and discussion

The performed experiments made it possible to obtain transparent YAG:Sm crystals in the direction of the crystallographic orientation [001] with the dimensions close to 70 mm × 25 mm × 115 mm, their color was light brown (Fig. 1). To study the distribution of samarium along the growth direction, there was used a polished plane-parallel plate made from the middle part of the crystal. The concentrations of samarium were measured by the methods of optical spectrophotometry using a spectrophotometer Optizen 3220 UV and energy dispersive *X*-ray fluorescence analysis (on

Elvax-Light, Elvatech). As reference samples, there was used optical ceramics YAG:Sm with different fixed samarium concentrations. It was found that in the obtained crystals the concentration of Sm^{3+} ions in the optical part ranged from ~ 3 at.% to 7.4 at.% .

Fig. 2 presents the results of studying the distribution of samarium in comparison with the theoretical calculation according to the Galliver-Pfann relation:

$$C = KC_0(1 - g)^{K - 1},$$

where *K* is the effective coefficient of the dopant distribution, C_0, the initial concentration of samarium in the melt, *g*, the share of the crystallized melt.

As seen from the figure, the obtained experimental values are in a very good agreement with the theoretical distribution calculation at the effective distribution coefficient *K*=0.32. This almost coincides with the results reported for the crystals obtained by the Czochralski method in [4].

Structure perfection in the crystals was investigated by the method of three-crystal *X*-ray diffractometry (XRD) in CuK$_{\alpha 1}$ radiation [13]. The samples were subjected to several stages of preparation (grinding, mechanical polishing, chemico-mechanical polishing) and had the crystallographic orientation (001) with an accuracy of ± 0.5°.

Scanning along the sample surface was realized parallel to the growth direction (the reflex <800>), perpendicular to the growth direction, with simultaneous record of the half-width values of the diffraction rocking curve β. As found while scanning the surface of the samples obtained from the rectangular part of the crystal (Fig. 2b), for the plane (001) with β of
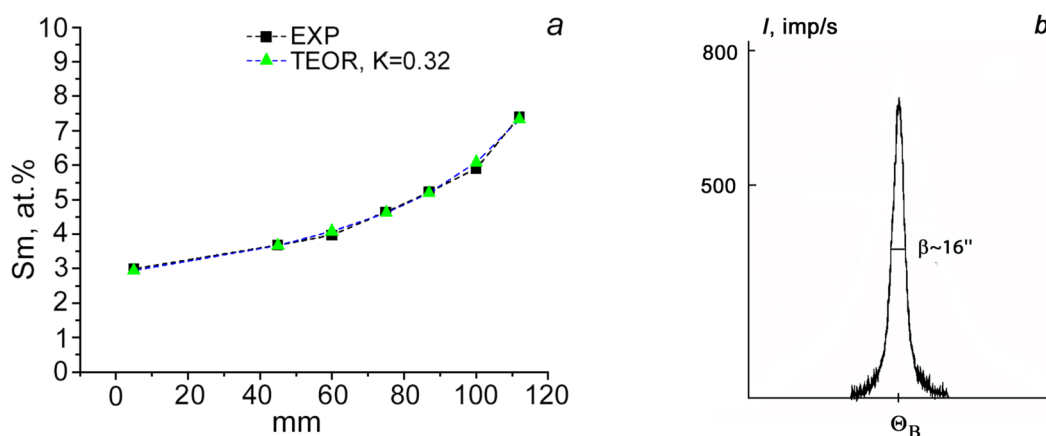

Fig, 2. a – Distribution of samarium ions in YAG:Sm crystals as against theoretical calculation; b - diffraction rocking curve for the reflex <800> of YAG:Sm crystal
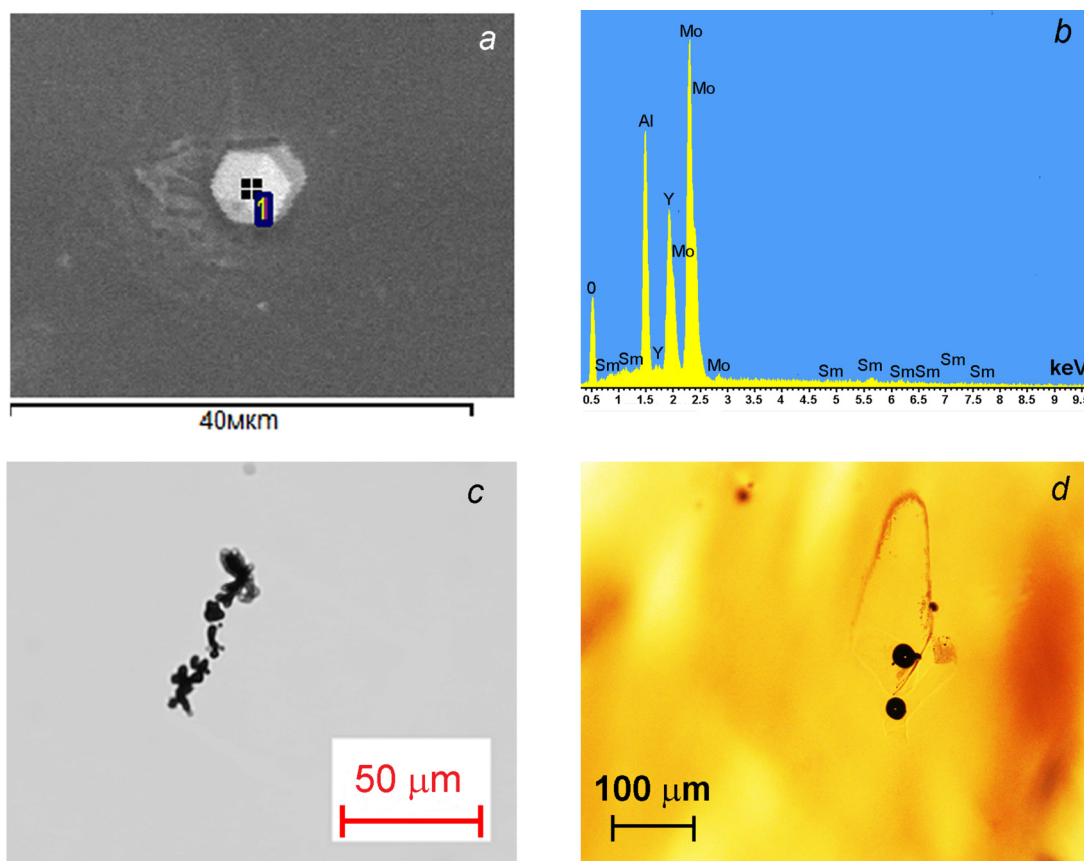
Fig. 3. Defects in YAG:Sm crystals grown by HDC method: *a* – SEM electron image of an inclusion on the base of construction materials (Mo and W); *b* – EDS spectrum of the said inclusion (point 1); *c* – optical image of an aggregate of micro-inclusions ; *d* – dislocation loop with a colony of inclusions

16 ang. sec, there was observed high uniformity of the distribution along the crystal length and thickness.

If to illuminate the grown crystal with laser beam (532 nm), there can be observed individual light-scattering centers and their clusters. Such centers may be distributed non-uniformly, their concentration and size may vary within rather wide range depending on the chosen crystallization conditions. There exist several types of defects that form such centers: gas pores, inclusions of the material of the thermal zone construction (heater, screens and crucible), as well of the crystal components.

Bubbles are identified most easily. since their dimensions are relatively large (≥ 0.1 mm). As a rule, in the crystal bulk individual bubbles are not observed, they are concentrating near the crucible walls.

The use of construction materials in the thermal zone, in particular, of tungsten heater and molybdenum crucible results in contamination of the crystal with these elements of the melt and formation of micro-particles on their base. Such inclusions have more or less regular shape and a size of $\sim 10 - 30$ µm. The studies of the morphology and EDS spectra by means of a scanning electron microscope of JSM-6390LV type and an energy dispersive AZtecEnergy X-maxN50 spectrometer made it possible to reveal the presence of construction materials in these inclusions (Fig. 3 *a,b*). Moreover, it was found that the crystals contained agglomerates of these micro-particles and inclusions of irregular shape (Fig. 3*c*). The shape of the microparticles is similar to that of MoO_3 crystals grown from the gas phase [14]. This fact makes it possible to assume the presence of molybdenum in these inclusions, as well as the mechanism of their formation due to mass transfer through the vapor-gas phase on the surface of the charge or the melt.

Besides simple homogeneous defects, there was revealed the presence of defects and inclusions with a complex structure, in particular, those that had a line or a pore framing a defect, in their vicinity (Fig. 3*d*). As is seen, such lines join and form more extended spatial structure that embraces several defects. Similar formations are observed in some other yttrium-aluminum crystals with other dopants, in particular, in YAG:Ce grown by
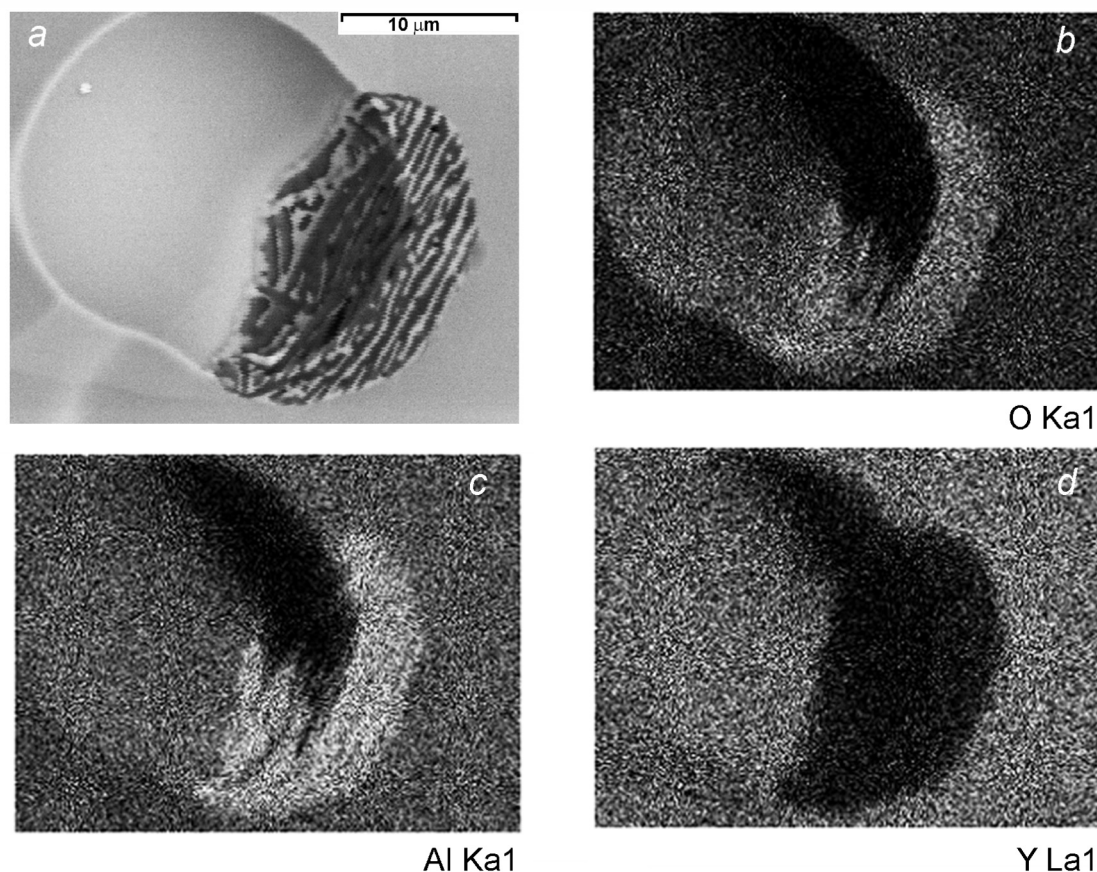
Fig. 4. SEM electron image of an eutectic inclusion in YAG:Sm (*a*) crystal and results of EDS mapping of this inclusion (*b, c, d*)

the HDC method as well as YAG:Nd, grown by the Czochralski method in iridium crucible [15] and GGG ($Gd_3Ga_5O_{12}$) crystals.

According to the model developed by J.W. Matthews et al. [16], inclusions trapped by the melt during solidification at further melt cooling give rise to a stress caused by differences in the thermal expansion of the matrix and the inclusion. This stress is partially relieved due to emergence and subsequent increase of dislocation loops near the inclusions. At the same time, while commenting on this model, E. Nes [17] admits that such defects occur due to precipitation of another phase leading to deformation of the matrix. This deformation decreases due to the appearance of one or several dislocation loops which in turn serve as places for the emergence of new, smaller defects (see Fig. 3 *d*). Thus, there may appear a flat colony of inclusions completely or partially surrounded by an edge dislocation.

In the grown crystals there may be also formed a complex defect in the form of precipitates of another phase in the pores (Fig. 4). According to the data of EDS mapping, the ra-

tios of the elements do not correspond to the theoretical ones for YAG. On the pore walls there are observed two-phase inclusions with excess of Al and deficiency of Y with respect to YAG, as well as characteristic layered or fibrous micro-structure. This may testify to the fact that the inclusions have an eutectic composition (most likely, consist of YAG and corundum). As a rule, such defects occur only within the end part of the crystal, and do not influence the overall quality of the main part. The content of carbon in all the investigated samples is close to the background value of the analysis, therefore, it can be concluded that carbon-containing inclusions are absent in the crystals.

Presented in Fig. 5 are the spectra of optical absorption of the obtained YAG:Sm crystals. These spectra contain thin lines corresponding to Sm^{3+} ions, as well as additional wide band absorption of a lower intensity with a center at 558 nm. The presence of an absorption band located near the above-mentioned band in yttrium-aluminum garnet was assumed in the theoretical work [18], where it was considered due to F^+ - centers.

Table 1. Optical characteristics of YAG:Sm crystals obtained by HDC method in molybdenum crucible in reducing carbon-containing medium

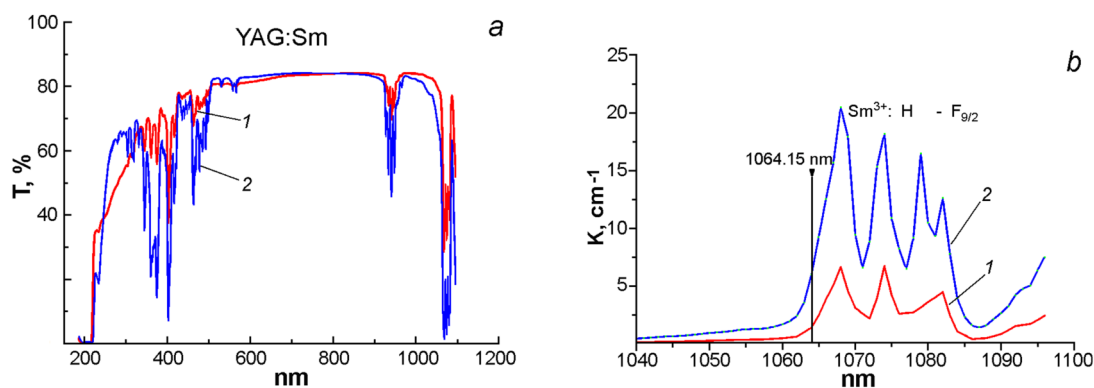| Crystal	Optical loss at 808 nm, cm^{-1}	Optical absorption at 1064 nm, cm^{-1}	FOM α(1064 nm)/α(808 nm)
Initial part	0.022	1.39	63.18
End part	0.015	5.94	396.00

Fig.5. Optical absorption spectra in the range of 190 -1000 nm (a) and near wavelength (1064.15 nm) of the main radiation line of YAG:Nd laser for 1- initial and 2- end part of YAG:Sm crystal (b).

Formation of color centers on the base of anion vacancies is possible due to the fact that the crystals have been grown in reducing medium. This is also evidenced by experiments on annealing of the crystals. After annealing in air (1500°C) the additional band disappears, and there remain only thin Sm^{3+} absorption lines caused by the transitions: $^6H_{5/2} \rightarrow ^4L_{13/2}$, $^6H_{5/2} \rightarrow ^6P_{5/2}$, $^6H_{5/2} \rightarrow ^4I_{15/2}$, $^6H_{5/2} \rightarrow ^4F_{5/2}$, $^6H_{5/2} \rightarrow ^4I_{11/2}$, $^6H_{5/2} \rightarrow ^4I_{9/2} + ^4M_{15/2}$, $^6H_{5/2} \rightarrow ^6F_{11/2}$, $^6H_{5/2} \rightarrow ^6F_{9/2}$ [19]. The most significant of them are the lines of Sm^{3+} ions that correspond to the transitions $^6H_{5/2} \rightarrow ^6F_{9/2}$ and are located near the main luminescence line of Nd^{3+} ions (1064.15 nm) in YAG lattice. In this range the line of Sm^{3+} absorption with a maximum at 1068 nm partially overlaps with the emission line of neodymium ions (Fig. 5b). Table 1 presents the optical characteristics of the obtained YAG:Sm crystals for the wavelengths of pumping (808 nm) and generation of YAG:Nd laser, as well as FOM of the crystals.

As is seen, the optical and spectral characteristics of the crystals are quite high in comparison with the parameters of YAG:Sm crystals obtained by different methods [3, 4, 6]. This testifies to the effectiveness of using YAG:Sm crystals grown by the method of HDC in molybdenum crucible in reducing carbon-containing medium in the capacity of suppressors of spontaneous luminescence in YAG:Nd.

4. Conclusions

The method of horizontal directional crystallization in molybdenum crucible using protective reducing Ar+(CO, H$_2$) atmosphere was applied to grow YAG:Sm single crystals with samarium concentration up to 7.4 at.%. The distribution of samarium ions along the crystal length fits well the Galliver-Pfann relation with the distribution coefficient $K = 0.32$. It is shown that the obtained crystals have high structure perfection and homogeneity that is characterized by the half-width of the swinging curve β of about 16 ang.sec for the crystallographic plane (001). The defects that lead to worsening of the optical quality and light scattering are found to be distributed in the crystal bulk non-uniformly. Except gas bubbles and micro-inclusions on the base of molybdenum and tungsten, there is revealed formation of complex defects with decorated dislocation loops and pores with eutectic inclusions.

In the optical absorption spectra of YAG:Sm crystals, in addition to thin lines of Sm^{3+} ions, there is also an additional absorption band at 558 nm, which arises as a result of reducing growth conditions. This absorption band corresponds to intrinsic defects bound up with anionic vacancies and the formation of F$^+$ color centers.

It is established that in the range that corresponds to the main luminescence band of neodymium ions (1064.15 nm) in YAG, the linear absorption coefficient reaches 6 cm^{-1}, and FOM is up to 400. This is quite enough for the use of the obtained YAG:Sm crystals as suppressors.

References

1. A. Lupei, V. Lupei, C. Gheorghe, A. Ikesue, *Romanian Reports in Physics*, **63**, 817, (2011). https://rrp.nipne.ro/2011_63_3/art18Lupei.pdf

2. R. Hub, R. Wilhelm, C. Kolleck et al., *Opt. Express* **18**, 13094, (2010). https://doi.org/10.1364/OE.18.013094

3. H. Yagi, J.F. Bisson, K. Ueda, T. Yanagitani, *J. Lumin.* **121**, 88 (2006).

4. H.-F. Li, J.-F. Han, G.-L. Yang, X.-G. Mo., *Journal of Synthetic Crystals,* **42**, 1305 (2013). http://rgjtxb.jtxb.cn/EN/Y2013/V42/I7/1305

5. M. Němec, J. Šulc, H. Jelínková et al., In: Proc. SPIE 11259, Solid State Lasers XXIX: Technology and Devices, 1125921 (2020). https://doi.org/10.1117/12.2544604

6. A.D. Timoshenko, O.O. Matvienko, A.G. Doroshenko et al., *Ceram. Int.* **49**, 7524 (2023). https://doi.org/10.1016/j.ceramint.2022.10.257

7. L.A. Oganesyan, V.Ya. Khaimov-Mal'kov, *J. Cryst. Growth* **52**, 530 (1981). https://doi.org/10.1016/0022-0248(81)90334-1

8. A. Ya. Dan`ko, N.S. Sidelnikova, G.T. Adonkin et al., *Funct. Mater.* **8,** 462 (2001).

9. S. Nizhankovskyi, S. Kryvonohov, N. Sidelnikova, *Cryst. Growth Des.*, **22**, 7153 (2022). doi.org/10.1021/acs.cgd.2c00822

10. S. V. Nizhankovsky, A. Ya. Dan'ko, Yu. V. Zorenko et al., *Physics of the Solid State,* **53** ,1, (2011) DOI:10.1134/S1063783411010215

11. S.V. Nizhankovskyi, O.O. Vovk, A.A. Kozlovskyi et al., *Opt. Mater.*, **141**, 113980 (2023) https://doi.org/10.1016/j.optmat.2023.113980

12. A. Ya. Dan`ko, N. S. Sidelnikova, G. T. Adonkin et al., *Funct. Mater.,* **10**, 217, (2003). http://funct-materials.org.ua/contents/10-2/FM102-28.pdf.

13. V. F.Tkachenko , M. A. Rom , A .A. Babichenko, *Instruments and Experimental Techniques,* **2**, 277, (1992).

14. S. Balakumar, H.C. Zeng, *J. Cryst. Growth*, **197**, 186, (1999). https://doi.org/10.1016/S0022-0248(98)00924-5

15. Deng Peizhen, Qiao Jingwen, *J. Cryst. Growth*, **82**, 579, (1987). https://doi.org/10.1016/S0022-0248(87)80001-5

16. J.W. Matthews, E. Klokholm, V. Sadagopan et al., *Acta Metallurgica*, **21**, 203, (1973). https://doi.org/10.1016/0001-6160(73)90005-9

17. E. Nes, *Scripta Met.*, **7**, 705, (1973) https://doi.org/10.1016/0036-9748(73)90117-8

18. J. Chen, T. C. Lu, Y.Xu et al., *J. Phys. Condens. Matter*, **20**, 325212, (2008). https://doi.org/10.1088/0953-8984/20/32/325212

19. M. Malinowski, R. Wolski, Z. Frukacz et al., *J. Appl. Spectrosc.,* **62**, 840, (1995) http://dx.doi.org/10.1007/BF02606647